Drug Design, Development and Therapy

Dovepress
open access to scientific and medical research

Open Access Full Text Article

ORIGINAL RESEARCH

Combining Network Pharmacology and Transcriptomics to Investigate the Mechanisms of Yujiang Paidu Decoction in the Treatment of Chronic Rhinosinusitis with Nasal Polyps

Yujie Li[1], Yadong Yin[2], Juan Xiong[3], Zhipeng Zhang[4], Linglong Li[3], Baoshun Zhang[4], Feng Zhang[3], Dehong Mao[3]

[1]College of Traditional Chinese Medicine, Chongqing Medical University, Chongqing, People's Republic of China; [2]Xijing Hospital, Air Force Medical University, Xi'an, People's Republic of China; [3]Department of Otorhinolaryngology, Yongchuan Chinese Medicine Hospital Affiliated to Chongqing Medical University, Chongqing, People's Republic of China; [4]College of Pharmaceutical Sciences, Southwest University, Chongqing, People's Republic of China

Correspondence: Feng Zhang; Dehong Mao, Email 164382044@163.com; 19m001@hospital.cqmu.edu.cn

Background: Yujiang Paidu Decoction (YJPD) has demonstrated clinical efficacy in the treatment of chronic rhinosinusitis. However, the effects and mechanisms of the YJPD on chronic rhinosinusitis with nasal polyps (CRSwNP) remain unclear.

Purpose: This study aimed to elucidate the potential mechanism of action of YJPD in the treatment of CRSwNP based on network pharmacology, transcriptomics and experiments.

Methods: A CRSwNP mouse model was established using ovalbumin (OVA) and staphylococcus aureus enterotoxin B (SEB) for 12 weeks and the human nasal epithelial cell (HNEpC) model was induced with IL-13 in vitro. Behavioral tests, scanning electron microscopy (SEM), micro-CT and pathological change of nasal tissues were observed to investigate the therapeutic effects of YJPD. Network pharmacology and transcriptomics were launched to explore the pharmacological mechanisms of YJPD in CRSwNP treatment. Finally, an ELISA, immunofluorescence, RT-qPCR, Western blotting and Tunel were performed for validation.

Results: Different doses of YJPD intervention effectively alleviated rubbing and sneezing symptoms in CRSwNP mice. Additionally, YJPD significantly reduced abnormal serological markers, structural damage of the nasal mucosa, inflammatory cell infiltration, goblet cell increases, and inhibited OVA-specific IgE levels and the secretion of Th2 cytokines such as IL-4, IL-5, and IL-13. Moreover, transcriptomics and network pharmacology analyses indicated that YJPD may exert anti-inflammatory and anti-apoptotic effects by inhibiting the MAPK/AP-1 signaling pathway. The experimental findings supported this conclusion, which was further corroborated by similar results observed in IL13-induced HNEpCs in vitro.

Conclusion: YJPD could alleviate inflammatory status and epithelial apoptosis by inhibiting aberrant activation of MAPK/AP-1 signaling pathway. This finding provides a strong basis for using YJPD as a potential treatment in CRSwNP.

Keywords: Yujiang paidu decoction, chronic rhinosinusitis with nasal polyps, network pharmacology, transcriptomics, inflammation

Introduction

Chronic rhinosinusitis with nasal polyps (CRSwNP), an important phenotype of chronic rhinosinusitis, caused by a variety of pathogenic factors and involves various diseases, which is characterized by a chronic inflammatory reaction in the nasal cavity and sinuses with a course of more than 12 weeks.[1] Currently, 2–4% adult global population suffers from CRSwNP.[2,3] Patients with CRSwNP often present with nasal obstruction, yellow purulent discharge, congestion, facial pain or pressure, and hyposmia or anosmia. CRSwNP has been diagnosed not only by the presence of nasal symptoms but must also be accompanied by evidence from objective diagnostic tools, such as nasal endoscopy or sinus CT.[4] Clinical studies have

Received: 15 March 2024
Accepted: 21 August 2024
Published: 27 August 2024

Graphical Abstract

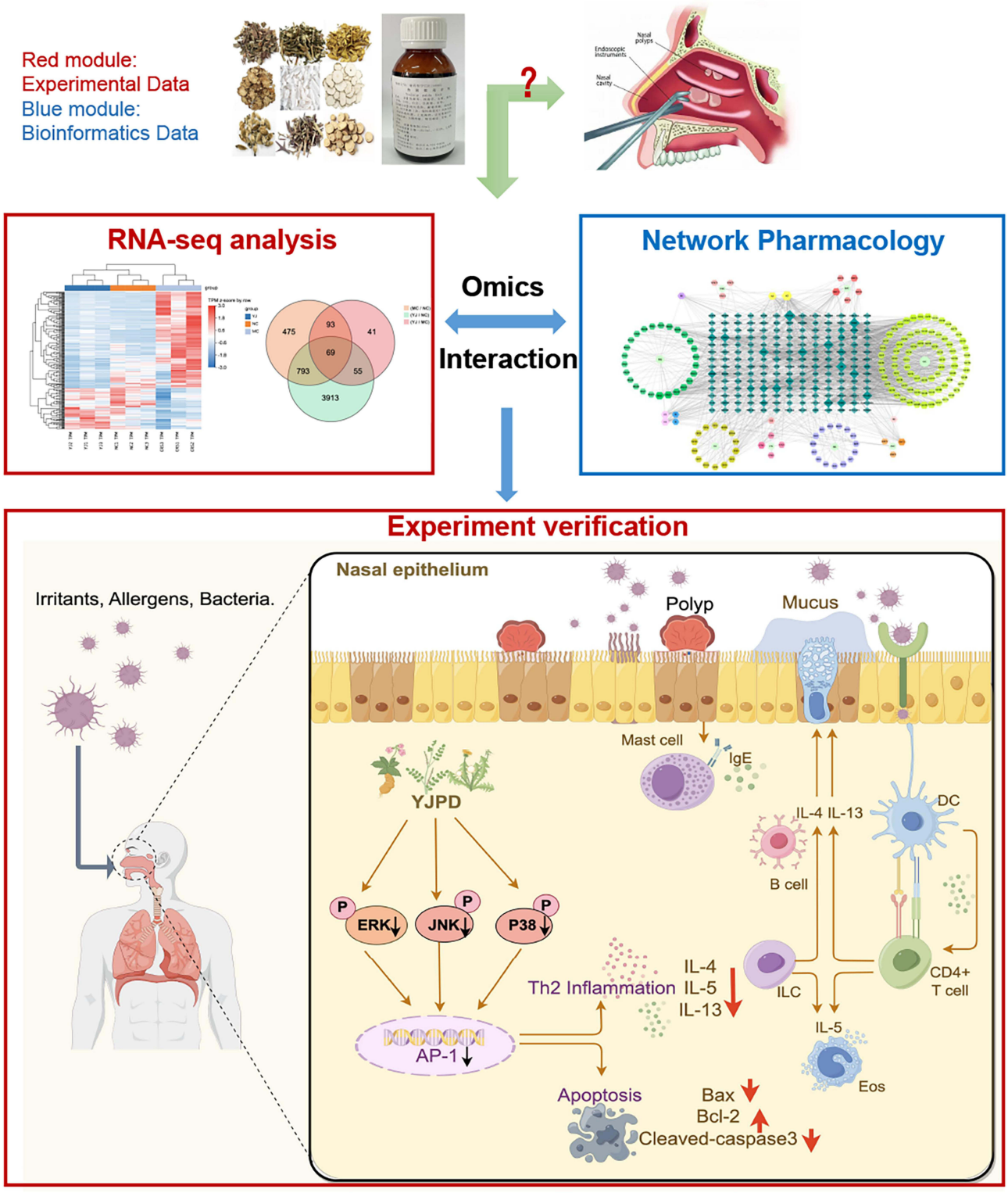

found that the prognosis of CRSwNP is not optimistic, and high rates of recurrence or relapse of nasal polyps after surgery can affect the daily life of patients and reduce their quality of life.[5]

In Western countries, CRSwNP is characterized by type 2 inflammation, including interleukin (IL)-4, IL-5 and IL-13, and polyps infiltrated by eosinophils, basophils and mast cells.[6] IL-4 and IL-13 promote antigen-specific Immunoglobulin E (IgE) production in B cells, and elevated IgE levels are also associated with eosinophilia.[2] Although type 1/3 inflammation is more common in Asian countries,[7] longitudinal reports suggest that the incidence of type 2 inflammatory CRSwNP has been increasing rapidly in some parts of Asia over the past decade.[8,9] The current main treatment methods for CRSwNP are based on glucocorticoid and sinus surgery. Multiple additional surgeries are often prescribed for patients with recurrence. Indeed, it currently does not have a "cure". Furthermore, Ordovas has already demonstrated that polyp basal cells would respond more strongly to IL-4/IL-13 cytokines than non-polyp basal cells, and the expression levels of IL-4/IL-13 are positively correlated with disease severity.[10] Therefore, inhibiting of Th2 cell activation might be a potential therapeutic strategy for CRSwNP.

Biologics previously developed for severe asthma or atopic dermatitis have been used in patients with CRSwNP, and more clinical data and experience are needed.[11] Novel therapies are urgently needed to improve disease, traditional Chinese medicine (TCM) has enormous potential in treating CRSwNP.[12] In TCM theory, sinusitis diseases caused by wind-heat in lung channel, heat-stagnation in the gallbladder-fu and phlegm stagnation in the nasal cavity. YJPD is derived from the classic formula Cang-Er -Zi-San,[13,14] a well-known TCM compound widely used in the treatment of chronic rhinitis, paranasal sinusitis and allergic rhinitis. Monarch drugs detoxify and discharge pus (*Houttuynia cordata Thunb*.[15] *Patrinia scabiosaefolia Fisch*.[16]). Minister drugs can enhance the power of monarch medicine to purge fu-organs to eliminate heat and detoxify (*Scutellaria baicalensis Georgi*,[17] *gypsum fibrosum*[18]). *Angelica dahurica (Fisch. ex Hoffm). Benth. et Hook*.[19] *Ligusticum chuanxiong Hort*.[20] *Magnolia biondii Pamp*.[21], *and Gleditsia sinensis Lam*.[22] are assistant drug relieving stuffy nose, expelling wind and alleviating pain. *Glycyrrhiza uralensis Fisch*.[23] moderating herb properties. In our previous study, we observed that the utilization of YJPD for oral or nasal irrigation yielded favorable outcomes in alleviating nasal congestion, purulent discharge, headache, and hyposmia among individuals diagnosed with chronic sinusitis.[24,25] We also found that YJPD can reduce the expression of GM-CSF, TNF-α and IL-8 in the mucosal tissue, improve the mucosal inflammatory environment, and thus attenuate damage to the nasal mucosal epithelium.[26] Therefore, it would be worthwhile to further investigate the mechanism of YJPD in the treatment of CRSwNP.

In TCM, multiple compounds are used, multiple targets are targeted, and multiple pathways are involved,[27] and network pharmacology research can provide insight into YJPD's complex mechanisms. Although network pharmacology has helped transform TCM from empirical medicine to evidence-based medicine, it is still confined to theoretical predictions. Considering the rigor of the experimental design, we adopted a comprehensive perspective of gene expression provided by transcriptomics and combined analysis of the results of the two omics to help confirm the potential mechanism of YJPD in the treatment of CRSwNP.

In this study, a classical OVA+ SEB-induced CRSwNP mouse model was used to investigate the therapeutic effects of YJPD at different doses. The efficacy of the YJPD was evaluated through comprehensive assessments of mouse behavior, SEM, micro-CT, and pathological sections. Through multi-omics analysis, we identified the potential anti-inflammatory and anti-apoptotic effects of YJPD via the MAPK/AP-1 pathways. Encouragingly, the in vitro and in vivo experiments verified these assumptions. In conclusion, our findings contribute to a comprehensive understanding of the mechanism of action underlying YJPD and lay a robust groundwork for its prospective utilization in the treatment of CRSwNP.

Materials and Methods

Reagents

Yujiang Paidu decoction (batch No.Z20150003) was obtained from the Chongqing Sanxia Yunhai Pharmaceutical Co.,Ltd. Ovalbumin (OVA; grade V) and aluminum hydroxide gels were purchased from Sigma-Aldrich (Shanghai, China). Staphylococcus aureus enterotoxin B (SEB) was obtained from Toxin (Sarasota, FL, United States). Dexamethasone was purchased from Solarbio (Beijing, China). Primary antibodies (phospho-ERK1/2, ERK1/2, phospho-p38, p38, phospho-JNK, and JNK) were purchased from CST (Cambridge, MA, USA). Recombinant human IL-13 was purchased from R&D Systems (Minneapolis, USA). The primary antibodies (c-FOS, Bax, Cleaved-caspase3, β-actin) and HRP-conjugated goat anti-rabbit

/mouse IgG were obtained from Proteintech (Wuhan, China). Primary antibodies (IL-4, IL-5, IL-13, and Bcl-2) purchased from Santa Cruz Biotechnology (Texas, USA).

YJPD Preparation and High-Performance Liquid Chromatography

The prescribed dosages of YJPD are shown in Table S1. Specifically, *Houttuynia cordata Thunb., Patrinia scabiosaefolia Fisch*. and *Magnolia biondii Pamp*. were distilled with water, approximately 500mL distillate was collected and the decoction was stored. Secondly, the residue was decocted with *Scutellaria baicalensis Georgi, Gypsum fibrosum., Gleditsia sinensis Lam., Ligusticum chuanxiong Hort., Angelica dahurica (Fisch. ex Hoffm). Benth. et Hook*. and *Glycyrrhiza uralensis Fisch*. in water three times: the first time for 80 min, the second and third times for 60 min, respectively. Finally, the decoction was mixed, filtered, concentrated, and ethanol was added to make the alcohol content of 70%. The ethanol was recovered and concentrated in a clear paste with a relative density of 1.20~1.25 (55~60°C). Double-distilled water was added into the above distillation solution to obtain a final volume of 100 mL and freeze-dried to obtain a powder. The powder was stored at −20°C until further use. Quality control standard of YJPD: Each per milliliter contains no less than 5mg of baicalin.

The chemical constituents of YJPD and the standards were determined using high-performance liquid chromatography (Agilent 1200 Series, Agilent Technologies, USA) with UV detector. The reference standards, quercetin, kaempferol, luteolin, baicalin, imperatorin and magnolin were purchased from Herbpurify Co., Ltd (Chengdu, China). The 20 mg/mL YJPD extracts were filtered through a 0.22-μm microporous membrane. Samples were passed through an Agilent ZORBAX Eclipse Plus C18 column (4.6 mm × 250 mm, 5μm) at a flow rate of 1 mL/min with the mobile phases of methanol (A) and 1% formic acid (B). Column separation was performed by a gradient elution program: 0–15 min, 20–50% A; 15–25 min, 50–25% A; 25–45 min, 25–95% A, 45–60 min, 95–20% A. The detection wavelength was 280 nm and the column temperature was 35°C.

Animal Model Establishment and Treatment

This study was supervised and approved by the Institutional Animals Care and Use Committee of Southwest University (Application Date: 10/06/2022, Ethics No.: IACUC-20220610-02). BALB/c mice (5 to 6-week-old, female) were obtained from Beijing Vital River Laboratory Animal Technology Co., Ltd. (Beijing, China), SPF grade, approval number: SCXK(Beijing)2021–0006, all mice were reared at 24°C with a 12-h light/dark cycle, and relative humidity was 55–65% in animal experimental center of Southwest University of Pharmaceutical Sciences College. After one week of adaptation, eighty mice were randomly divided into five groups: control (CON), chronic rhinosinusitis with nasal polyps (CRSwNP), dexamethasone (DEX, 1mg/kg), low dose YJPD (YJPDL, 3.9mL/kg), and high dose YJPD (YJPDH, 15.6mL/kg).

For the CON group, mice were administered intraperitoneal injections of phosphate-buffered saline (PBS) (200μL per mouse) on days 1 and 5, one week after the second intraperitoneal injection, mice were intranasally instilled with PBS (20 μL per mouse) for seven consecutive days. Subsequently, nasal instillation of PBS was performed three times per week from days 19 to 103. In the last eight weeks of the experiment, the mice received intragastric administration of 200μL normal saline.(2) In the CRSwNP group,[28] mice received intraperitoneal injections of 25μg OVA dissolved in 200μL PBS, in the presence of 2 mg aluminum hydroxide gel as an adjuvant on days 1 and 5. Model mice obtained nasal instillation with 6% OVA (20μL per mouse) daily from days 12 to 19 and prolonged continuous inflammation was maintained three times weekly from days 19 to 103. By the subsequent nasal exposure to 10ng SEB diluted in 20μL PBS with intranasal route once per week from days 49 to 103. During that period, mice received intragastric administration of 200μL normal saline. (3) In the DEX, YJPDL and YJPDH group, as a preventive intervention, before SEB exposure, mice received the same treatments as the CRSwNP group. After that, they were administered intraperitoneally 1mg/kg DEX, orally administered with 3.9mL/kg and 15.6mL/kg Yujiang Paidu decoction.

Blood Sample and Serum Collection

After mice were anesthetized with isoflurane, blood samples were harvested from retro-orbital plexus. A portion of the blood was used for routine blood (Mindray, Shenzhen, China), while the remainder was centrifuged (3000 rpm, 15 min) to obtain serum.

Nasal Lavage Fluid (NALF) Collection

A catheter was inserted into the nasopharyngeal region of each mouse and 500 μL of PBS. The NALF from the nostril were collected and centrifuged (1000 × g, 10 min, 4°C) to obtain the supernatant.

Micro-CT Scanning

Before the end of the experiments, all mice were undergone a nasal cavity micro-CT scan (Viva CT40, Scanco Medica, Switzerland) according to their anatomic localization.

Scanning Electron Microscope

We performed cardiac perfusion and dissected the nasal septum mucosa of mice under a stereoscopic microscope following the steps described in JoVE's article.[29] The 4*3mm^2 side close to the nasal septum was selected and fixed by immersion in 1% osmic acid 0.1M PBS. The specimens were then flushed 3 times in 0.1M phosphoric acid buffer and dehydrated in the increasing concentrations of alcohol. Finally, the mucosa was dried and coated with gold in MC1000 sputter coater (Hitachi, Tokyo, Japan), electron microscope SU8100 (Hitachi, Tokyo, Japan) used for analysis.

Enzyme-Linked Immunosorbent Assay

IL-4, IL-5, IL-13, and OVA-specific IgE levels were measured using ELISA kits, according to the manufacturer's instructions (CUSABIO, Wuhan, China). Data represent the average of at least five independent samples, each performed in triplicate.

Data Mining for Network Pharmacology

The active ingredients and corresponding targets of YJPD were obtained from the Traditional Chinese Medicine Systems Pharmacology Database and Analysis Platform (TCMSP, https://www.tcmsp-e.com/) and Swiss Target Prediction (http://www.swisstargetprediction.ch). We supplemented gypsum with the Bioinformatics Annotation database for Molecular mechANism of Traditional Chinese Medicine (http://bionet.ncpsb.org.cn/batman-tcm/) database. We further investigated the targets for chronic rhinosinusitis with nasal polyps were obtained from three databases: the Genecards (https://www.genecards.org) database and Online Mendelian Inheritance in Man (https://www.omim.org/) database.

The STRING (https://www.string-db.org/) database was used to construct the PPI network of common potential target genes of YJPD and CRSwNP and the parameters with high confidence (0.9). The PPI network was imported into Cytoscape (version 3.2.1) for further analysis. Finally, GO and KEGG analysis the common genes were performed using the DAVID (https://david.ncifcrf.gov/home.jsp) database.

Transcriptome Sequencing

An amplified cDNA library was constructed from the total nasal mucosa RNA and each library was sequenced on the BGIseq500 platform. Differential expression between the two comparison combinations was analyzed using the DESeq under the conditions of Fold Change ≥2 and Adjusted P value ≤0.001. Then, the differential genes were functionally classified according to GO and KEGG annotation results and the phyper (https://en.wikipedia.org/wiki/Hypergeometric_distribution) in R software was used for KEGG enrichment analysis, as potential pathway for the transcriptomics analysis of YJPD in treatment with CRSwNP.

Cellular Culture

HNEpC cells were obtained from the BeNa Culture Collection (Beijing, China) and cultured in MEM/EBSS (Hyclone, Logan, UT, USA) medium with 10% fetal bovine serum (GIBCO, Grand Island, NY, USA), at 37◦C with 5% CO_2 cultivated. A model of nasal epithelium was fabricated in vitro to investigate whether YJPD could ameliorate

inflammation and apoptosis, the cells were treated with YJPD (200 or 400 μg/mL) for 30 min, and then stimulated with 10 ng/mL recombinant human IL-13 for 24 h.[30]

Histopathology Analysis and Immunofluorescence Staining

Nasal mucosal tissues from mice were fixed, embedded and made into paraffin sections, subjected to hematoxylin and eosin (H&E), toluidine blue (TB) and periodic acid Schiff (PAS). For immunofluorescence staining, the paraffin-embedded nasal tissue was dewaxed and hydrated. Antigen repair was performed by boiling the slides in Sodium Citrate Antigen Retrieval Buffer (pH 6.0) at 95–100°C for 10 minutes. The sections were plugged with 10% goat serum and incubated at 37°C for 0.5 h. Anti-c-FOS was used as the primary antibody incubated overnight at 4°C, and the slides were incubated with an anti-mouse horseradish peroxidase-conjugated secondary antibody for 1 hour at 37°C. After that, the slides were washed with PBS for 3 times, and the tissue was sealed with a tablet containing DAPI. Anti-fluorescence agent was added and observed with a fluorescence microscope (Nikon ECLIPE Ci, Tokyo, Japan). Data represent an average of six independent samples, each performed in triplicate.

TUNEL and Annexin V-FITC Apoptosis Assays

Apoptosis assays were performed using the TUNEL kit (C1086, Beyotime Biotechnology, Shanghai, China) and Annexin V-FITC/PI Apoptosis Kit (E-CK-A211, Elabscience, Wuhan, China) following the manufacturer's instructions. The results were visualized by fluorescence microscope and flow cytometry (BD FACSCalibur, San Diego, CA, USA), respectively. The data represent an average of six independent experiments, each performed in triplicate.

Real-Time Quantitative PCR

Extraction of total RNA from nasal mucosal tissue was performed with AG RNAex Pro reagent (Accurate Biology, ChangSha, China). The obtained mRNA concentration was transformed into cDNA using the FastKing cDNA kit with gDNase (TIANGEN BIOTHCH, Beijing, China). Synthesized cDNA was amplified by SuperReal PreMix Plus SYBR Green Kit (TIANGEN BIOTHCH, Beijing, China). All primers sequences are listed in Table S2. The expression of the target gene (IL-4, IL-5, and IL-13) relative to the β-actin was calculated by $2^{-\Delta\Delta CT}$. Roche LightCycler96 System was used for qPCR analysis. The data represent an average of six independent experiments, each performed in triplicate.

Western Blotting

Proteins were extracted from mouse nasal mucosa tissues and HNEpCs by using lysates and protease inhibitors. After electrophoretic separation, the proteins were transferred onto NC membranes. Membranes blocked with 5% skim milk for 1h and probed with the primary antibodies overnight at 4°C. The membranes were further incubated for 1h with secondary antibodies. Each incubation step was followed by three washes with TBST. After chemiluminescence, the relative protein expression was analyzed using ImageJ software. Six independent mice samples and three independent cell experiments with technical triplicate.

Statistical Processing

Data are expressed as mean ± standard error of the mean (SEM). Statistical analysis was conducted using a one-way analysis of variance (ANOVA) followed by Tukey's post hoc test. Statistical analysis and visualization were performed using GraphPad Prism 8. $P<0.05$ was considered statistically significant.

Results

YJPD Attenuates Nasal Mucosal Inflammation in CRSwNP Mouse Model

To investigate whether YJPD had any therapeutic effect on CRSwNP, a mouse model of the normal group, model group, positive control DEX (1mg/kg) group, YJPDL(3.9mL/kg) and YJPDH (15.6mL/kg) groups was successfully established (Figure 1A). Within 10 minutes of the final intranasal challenge with OVA+SEB, the frequency of sneezing and nose rubbing were measured. The results showed that the numbers of sneezing and rubbing decreased dramatically in YJPD

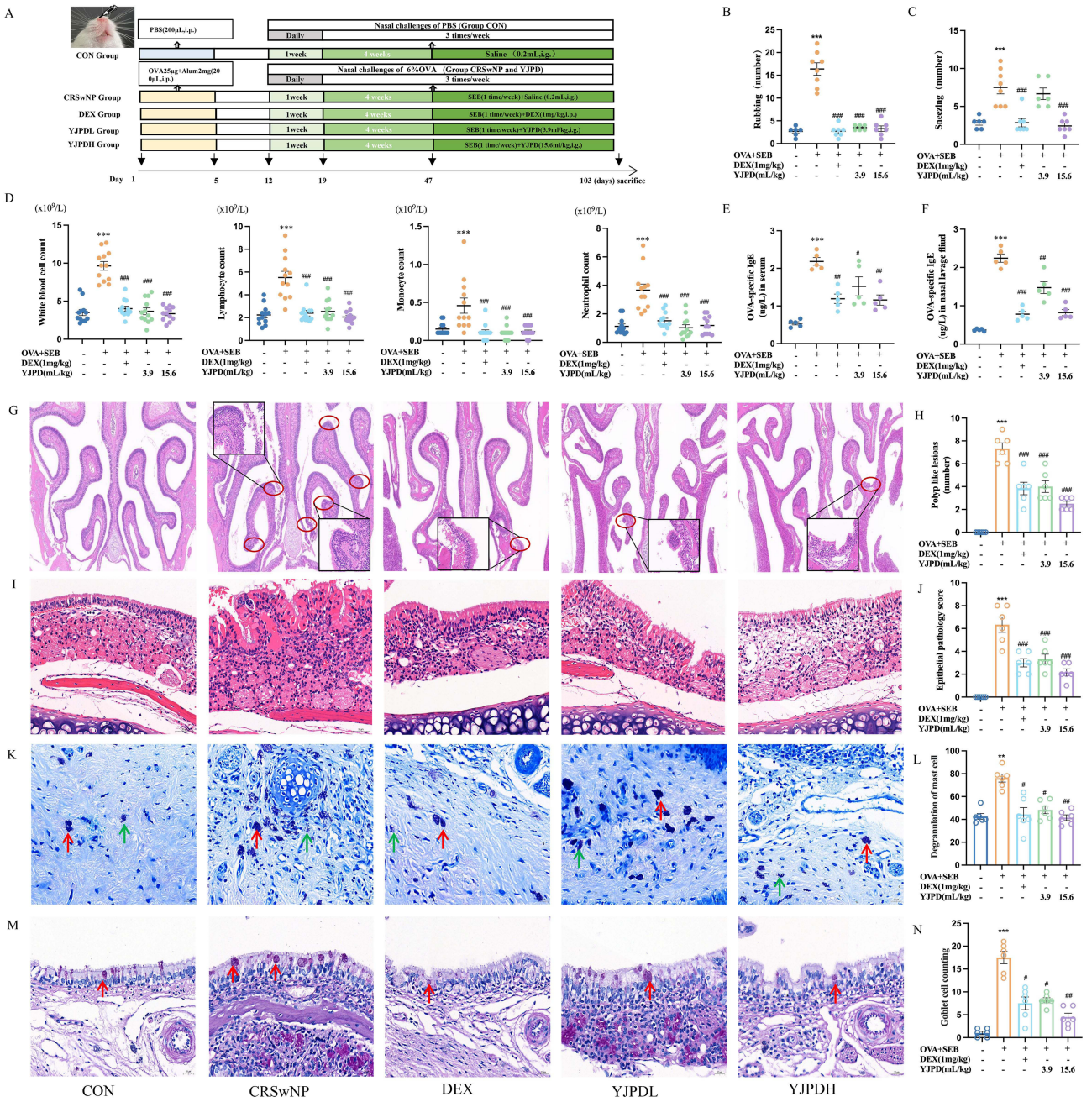

Figure 1 YJPD attenuates nasal mucosal inflammation in CRSwNP mouse model. (**A**) A protocol of the murine model of chronic rhinosinusitis with nasal polyps and treatment. (**B** and **C**) The frequency of rubbing and sneezing. (**D**) The number of various leukocytes were counted from the blood. (**E** and **F**) OVA-sIgE levels in serum and NALF were measured by ELISA. (**G** and **H**) Red circles indicated polypoid lesions. (**I** and **J**) HE staining and epithelial pathological score. (**K** and **L**) TB staining and number of mast cells (red arrows), degranulated mast cells (green arrows). (**M** and **N**) PAS staining and goblet cells (red arrows) counting. scale bar=20um (400X). $^{**}p < 0.01$, $^{***}p < 0.001$ versus CON; $^{\#}p < 0.05$, $^{\#\#}p < 0.01$, $^{\#\#\#}p < 0.001$ versus CRSwNP.

group compared with the model group (Figure 1B and C), suggesting that YJPD decoction could effectively improve sinusitis symptoms in CRSwNP mice.

Infiltration of inflammatory cells strengthens the induction of airway and nasal inflammation.[1] To further assess the effects of YJPD on inflammatory response, the measurement of peripheral blood cells were performed. As shown in Figure 1D, compared with the normal group, total white blood cells, lymphocytes (Lym), monocyte (Mono) and neutrophils (Neu) were notably increased in CRSwNP group ($p<0.001$), and YJPD treatment reversed these indicators to near normal levels ($p<0.001$), contributing in a concentration dependent effect. Furthermore, in the detection of OVA-

specific IgE in serum or NALF (Figure 1E and F), both doses of YJPD, especially 15.6 mL/kg YJPD, markedly decreased anti-OVA sIgE level in CRSwNP mice, which was similar to DEX (p<0.01).

Evaluation of Nasal Mucosa Pathology in CRSwNP Mice

The number of polypoid lesions indicated that CRSwNP mice model was successfully established. YJPDH can significantly reduce polyps, with effects superior to those of the positive control drug dexamethasone (Figure 1G and H). *H&E sta*ining revealed that the nasal septum tissues of the CRSwNP group were densely infiltrated with inflammatory cells, glandular hyperplasia, hyalinization of mucosal epithelial cells, and eosinophilic bodies in the cytoplasm (Figure 1I). DEX, YJPDL and YJPDH treatment reduced inflammatory cell infiltration, the epithelial pathology score showed statistical significance (Figure 1J) (p<0.001). TB staining revealed more mast cells in the CRSwNP group than in the control group (p< 0.05), while the number of mast cells in DEX group (p< 0.05), YJPDL group and YJPDH group decreased (p< 0.05), and there was no difference between the three groups (Figure 1K and L). The model group mice's nasal goblet cell (GC) proliferation revealed by PAS staining, suggesting that DEX, YJPDL, and YJPDH treatment could reduce mucus production (Figure 1M and N). Taken together, the above results showed that YJPD ameliorates nasal mucosal inflammation in the CRSwNP mouse model.

YJPD Ameliorates Nasal Mucociliary Damage

The nasal mucosa in the CON group had a normal ciliary structure, a large number of neatly placed ciliated cells (CC), and close intercellular spacing. In CRSwNP group, the number of CC was reduced, the arrangement was sparse, slightly shrunken and collapsed, the intercellular space was widened, and the cell base was exposed. Damage to cilia (Cil) impaired the ciliary clearance system's defenses against foreign pathogen invasion and encouraged foreign substances adhesion on the mucosal surface. The increasing GC leads to accelerated mucus secretion and decreased mucus excretion of mucosal epithelium.[31] The damage to the nasal mucosa were reversed in the DEX and YJPDL groups; especially, in the treatment of YJPDH group, GC were rarely detected and Cil were dense and covered almost all mucosal surfaces, and their length was basically the same (Figure 2). These findings implicate Cil injury can aggravate the inflammation of nasal mucosa, which can be reversed by YJPD.

YJPD Alleviates Polyp Formation in the CRSwNP Mouse Model

We found that coronal CT scan images (Figure 3) were consistent with histological findings. The CON group showed smooth and thin mucosa on micro-CT, whereas the CRSwNP group exhibited uneven mucosal surfaces, including diffuse mucosal thickening of the nasal septum, maxillary sinus, and ethmoidalis (yellow arrow). In contrast, the nasal mucosae of the intervention group mice were smoother than that of the CRSwNP group, with unobstructed nasal cavity and reduced polypoid tissue.

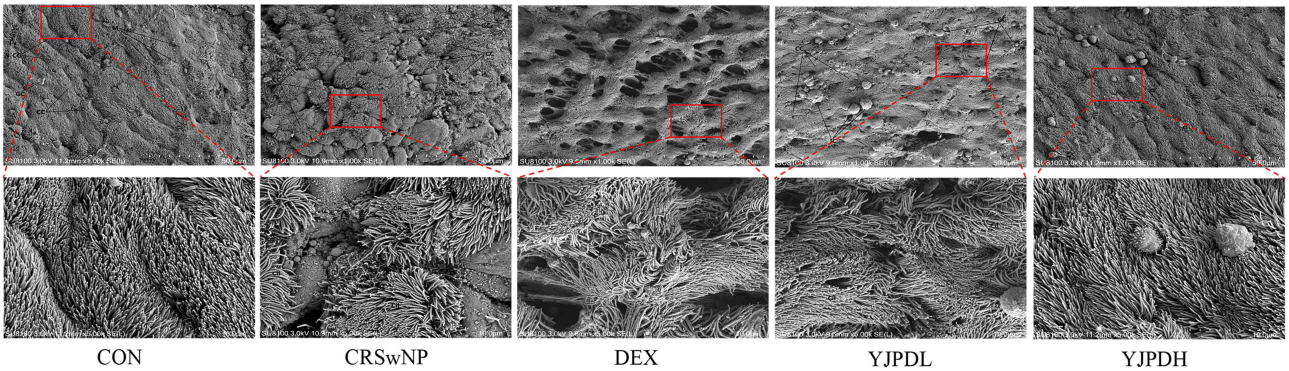

Figure 2 Scanning electron microscopy of isolated nasal septa from mice. In CON group the number of CC was more, and the Cil structure was normal. In CRSwNP group, the nasal mucosa was most damaged, the amount of CC was sharply reduced and Cil was largely degraded. GC increased, and a large area of mucus (M) was observed on the surface of epithelial cells. The nasal mucosal injury of DEX, YJPDL and YJPDH was relatively relieved. scale bar=10um (10000X).

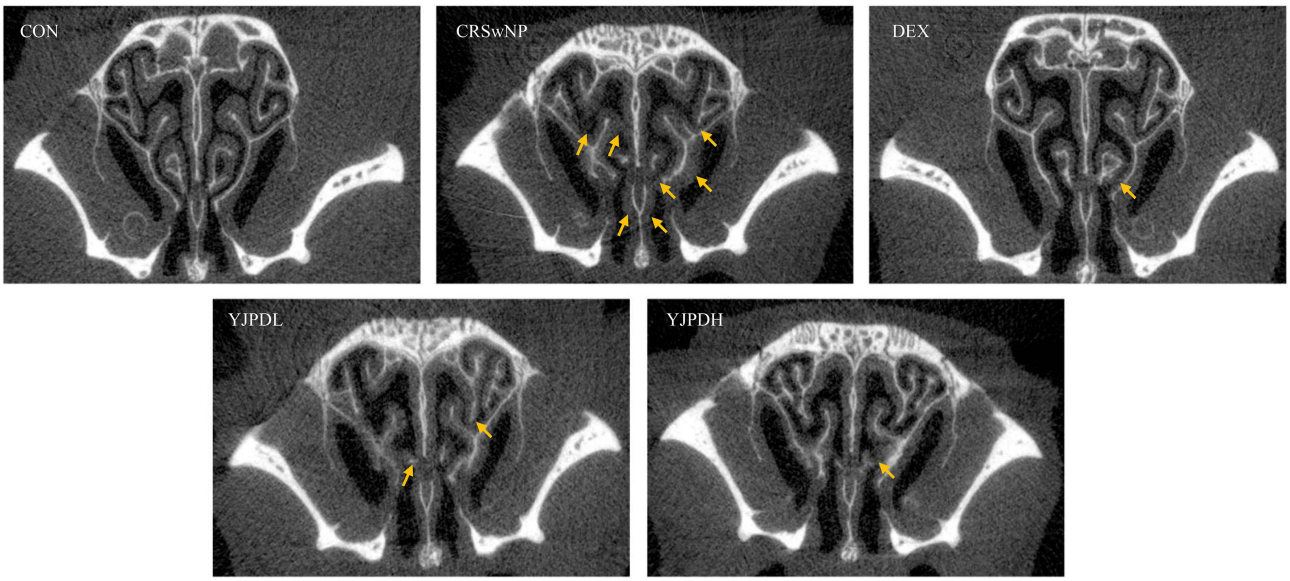

Figure 3 Micro-CT scan of isolated nasal septa from mice. Yellow arrow indicates uneven and diffusely swollen mucosa.

Network Pharmacology Analysis of YJPD in the Treatment of CRSwNP

Traditional Chinese medicine prescriptions have the characteristics of multi-components, multi-targets and many pathways. Effective compounds and potential active ingredient candidates (oral bioavailability≥30%, drug-like≥0.18) in YJPD were collected from the TCMSP database. We screened a total of 185 compounds and identified 182 target genes (Table S3). We made a pairwise comparison of each traditional Chinese medicine to find out the important components (Quercetin and Kaempferol) (Table S4), which were also identified by HPLC (Figure S1). In addition, the Chinese medicine-active ingredient-target network was constructed to illustrate directly (Figure 4A).

We also identified 949 CRSwNP target genes from the databases and 50 overlapping common protein targets were obtained between YJPD and CRSwNP by taking the intersection (Figure 4B). These common targets were used for protein-protein interaction (PPI) analysis and which were consisted of 50 nodes and 618 edges (Figure 4C). A cluster analysis of these genes further confirmed YJPD's efficacy, and the first cluster (AKT1, BAX, BCL2, CASP3, CASP8, CASP9, and CHRM3) was mainly involved in apoptosis. The top 20 targets obtained using the betweenness algorithm are shown in Figure 4D.

Figure 5 shows the results of GO and KEGG enrichment analysis. The most enriched BP terms (Figure 5A and B) were associated with apoptosis, including neuron apoptotic process, apoptotic process and negative regulation of apoptotic process. Moreover, inflammatory response also played an important role in BP. The CC and MF showed in Figure S2. KEGG analysis showed that the mechanism of how YJPD acts might be associated with IL-17 signaling pathway, MAPK signaling pathway and apoptosis pathway (Figure 5C and D).

Transcriptomics Revealed the Signaling Pathways Associated with YJPD in the Treatment of CRSwNP

To systematically assess the mechanism of YJPD in CRSwNP treatment, the transcriptomics of the control (NC), CRSwNP (MC), and YJPDH (YJ) groups were analyzed using the DNBSEQ platform (three nasal mucosa tissue samples each group). Figure 5E indicates that there are 162 differential expressed genes (DEGs) in the MC group and the YJ group (Fold Change ≥2, Adjusted P value ≤0.001). Principal component analysis (PCA) separated samples from NC and MC groups, and YJ samples were closer to NC samples, indicating that YJPD could return normal levels to genes altered during CRSwNP (Figure S3). Comparing the MC group to the NC group, 855 DEGs were up-regulated and 575 were down-regulated (Figure 5F), whereas 77 up-regulated and 181 down-regulated genes were discovered in the MC group compared with the YJ group (Figure 5G). Finally, we used the DEGs to draw a heatmap (Figure 5H).

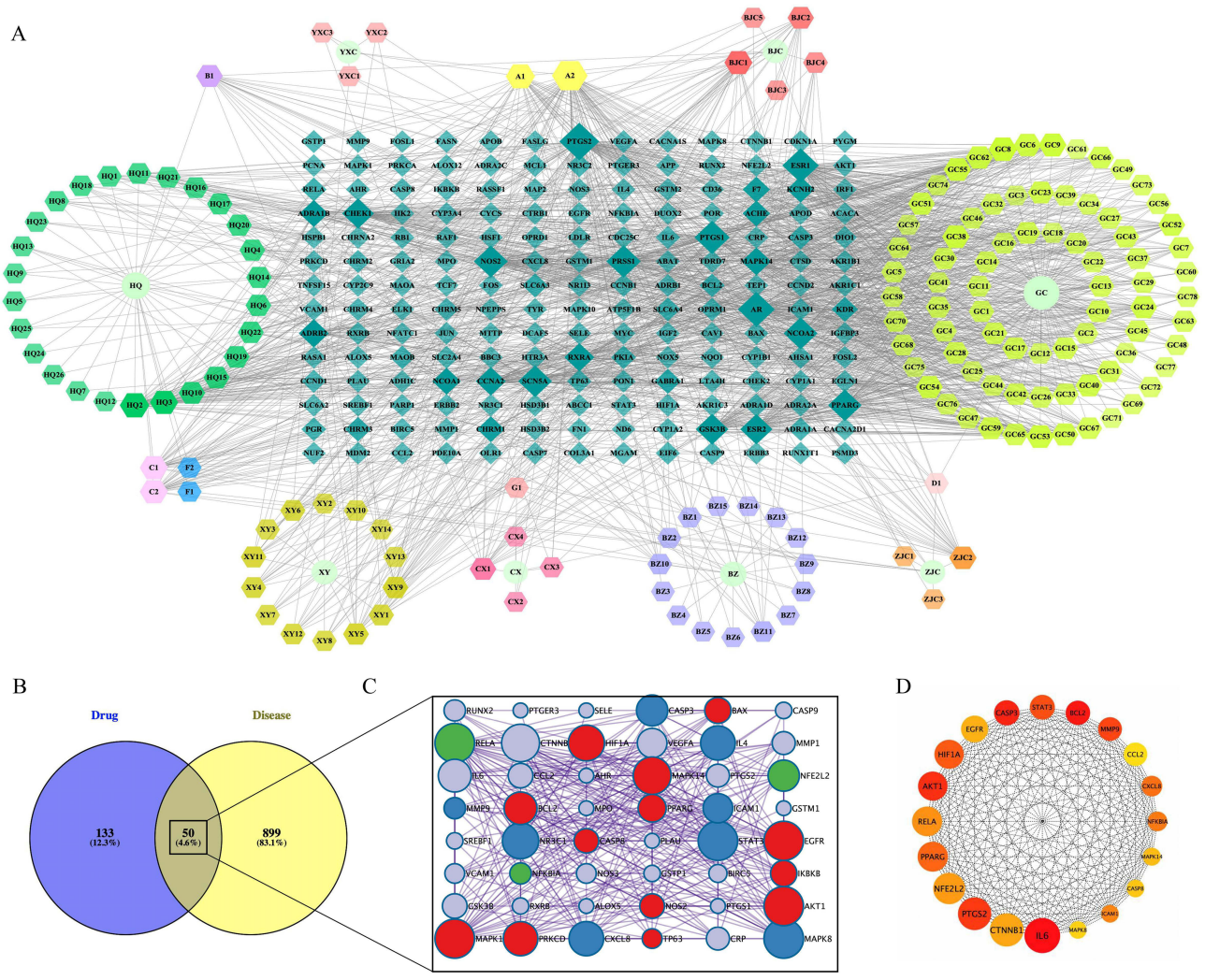

Figure 4 Pharmacological network construction for YJPD treating CRSwNP. (**A**) The network of "Drugs-active compounds-potential targets". Circles of green, hexagons of various colors, and diamonds of blue represent TCM, compounds and predicted targets, respectively. (**B**) Venn diagram of targets common to YJPD active ingredients and CRSwNP. (**C**) The four clusters screed by MCODE analysis. (**D**) Top 20 target proteins screened by CytoHubba.

Results of GO enrichment showed a high degree of enrichment in DEGs related to inflammatory response, negative regulation of endothelial cell apoptotic process, and transcription factor AP-1 complex (Figure S4). KEGG analysis revealed that the top several pathways were mainly associated with inflammation, YJPD may interfere with CRSwNP through TNF signaling pathway, IL-17 signaling pathway, MAPK signaling pathway and apoptosis signaling pathway, etc. (Figure 5I).

YJPD Inhibits Inflammatory Cytokines via MAPK/AP-1 Signaling Pathway

Integrating the results of network pharmacology and transcriptomics, we used Western blotting to evaluate the phosphorylation of p38, JNK and ERK related proteins in the MAPK pathway. We demonstrated that the YJPD downregulated the phosphorylation levels of p38, JNK and ERK MAPK compared with CRSwNP group (Figure 6A). Previous studies have shown that the intracellular localization and transcriptional activity of c-FOS are tightly regulated. In particular, transcriptional activity can be enhanced by the phosphorylation of various serine and threonine. Combined with transcriptomics, c-FOS drew our attention due to its marked upregulation in the model group and obvious downregulation in YJPD group. Consistent with this, we validated with Western blotting and immunofluorescence and obtained similar results (Figure 6B and C). In addition, ELISA (Figure 6D), RT-qPCR (Figure 6E) and Western blot analysis (Figure 6F) were performed to detect Th-2 associated cytokine levels, and the results showed that the levels of

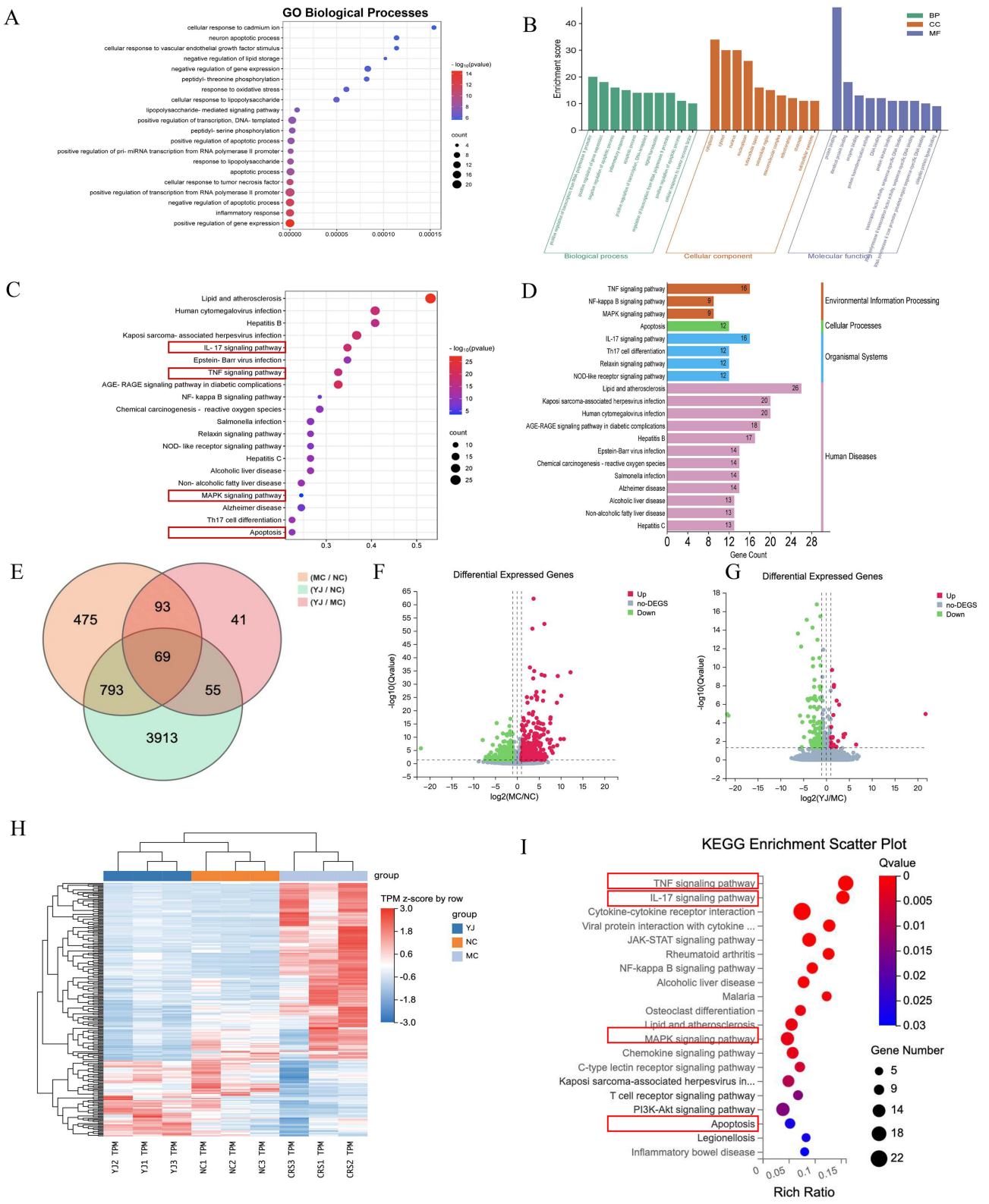

Figure 5 The transcriptome data and network pharmacology screens key pathways for YJPD treating CRSwNP. (**A** and **B**) GO enrichment analysis and its classification of BP, CC and MF. (**C** and **D**) The top 20 KEGG pathways and classification. (**E**) Venn diagram showing the common target proteins between NC, MC, and YJ. (**F** and **G**) DEGs volcano map of MC vs NC and YJ vs MC. The red dots refer to upregulated genes. The green dots refer to down-regulated genes. (**H**) Heat map of DEGs in YJ vs MC vs NC. (**I**) Pathway enrichment analysis of 162 key genes by KEGG.

https://doi.org/10.2147/DDDT.S461769 DovePress

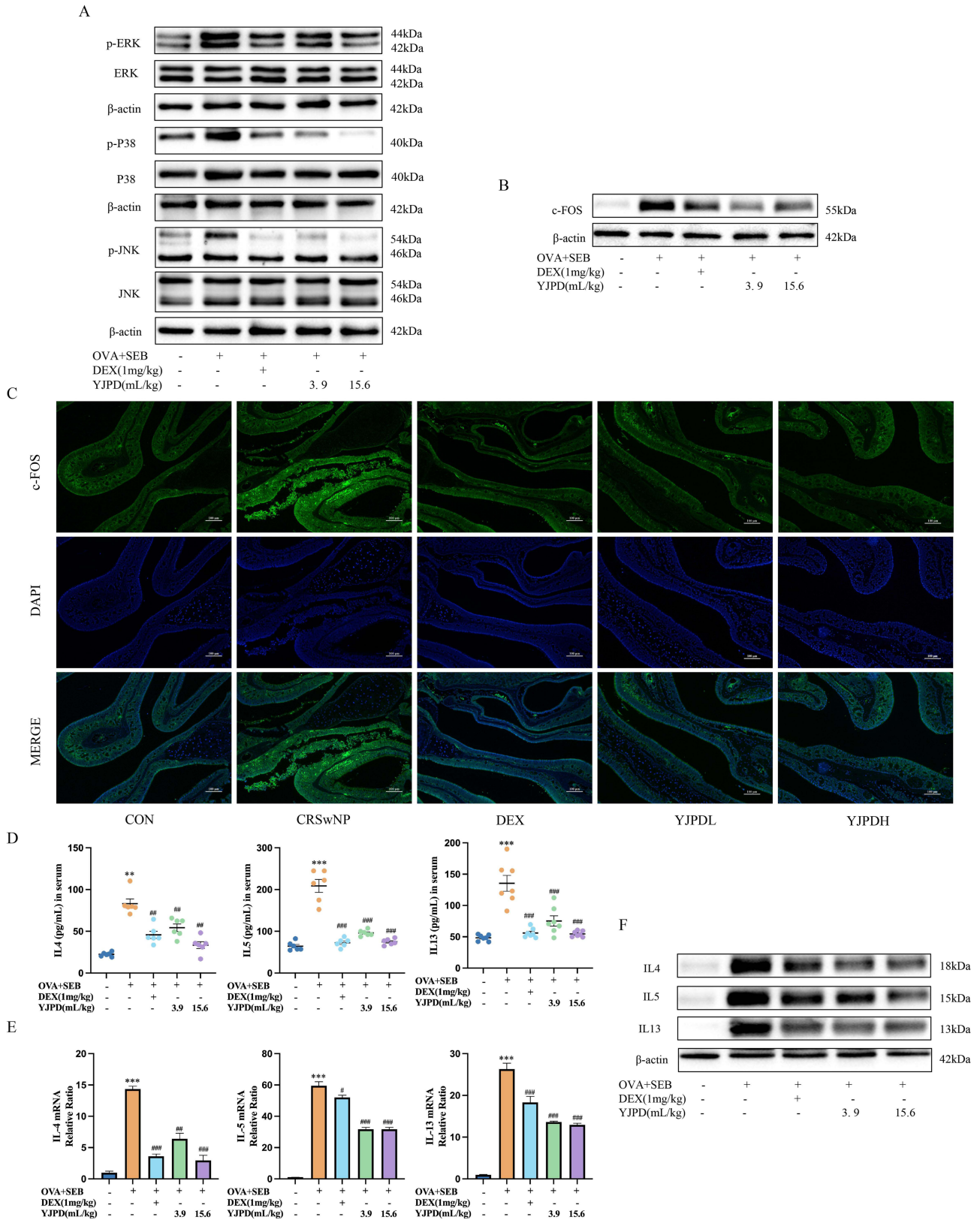

Figure 6 YJPD inhibits inflammatory cytokines via MAPK/AP-1 signaling pathway in CRSwNP mice. (**A**) Western blots of phospho-ERK1/2, ERK1/2, phospho-P38, P38, phospho-JNK, JNK in nasal mucosa of mice. (**B**) Western blots and (**C**) immunofluorescence of c-FOS in nasal tissues of mice. (**D**) Secretion levels of IL-4, IL-5 and IL-13 in blood serum were detected by Elisa. (**E**) RT-qPCR and Western blot (**F**) of IL-4, IL-5 and IL-13 in the nasal mucosa samples. $^{**}p < 0.01$, $^{***}p < 0.001$ versus CON; $^{\#}p < 0.05$, $^{\#\#}p < 0.01$, $^{\#\#\#}p < 0.001$ versus CRSwNP.

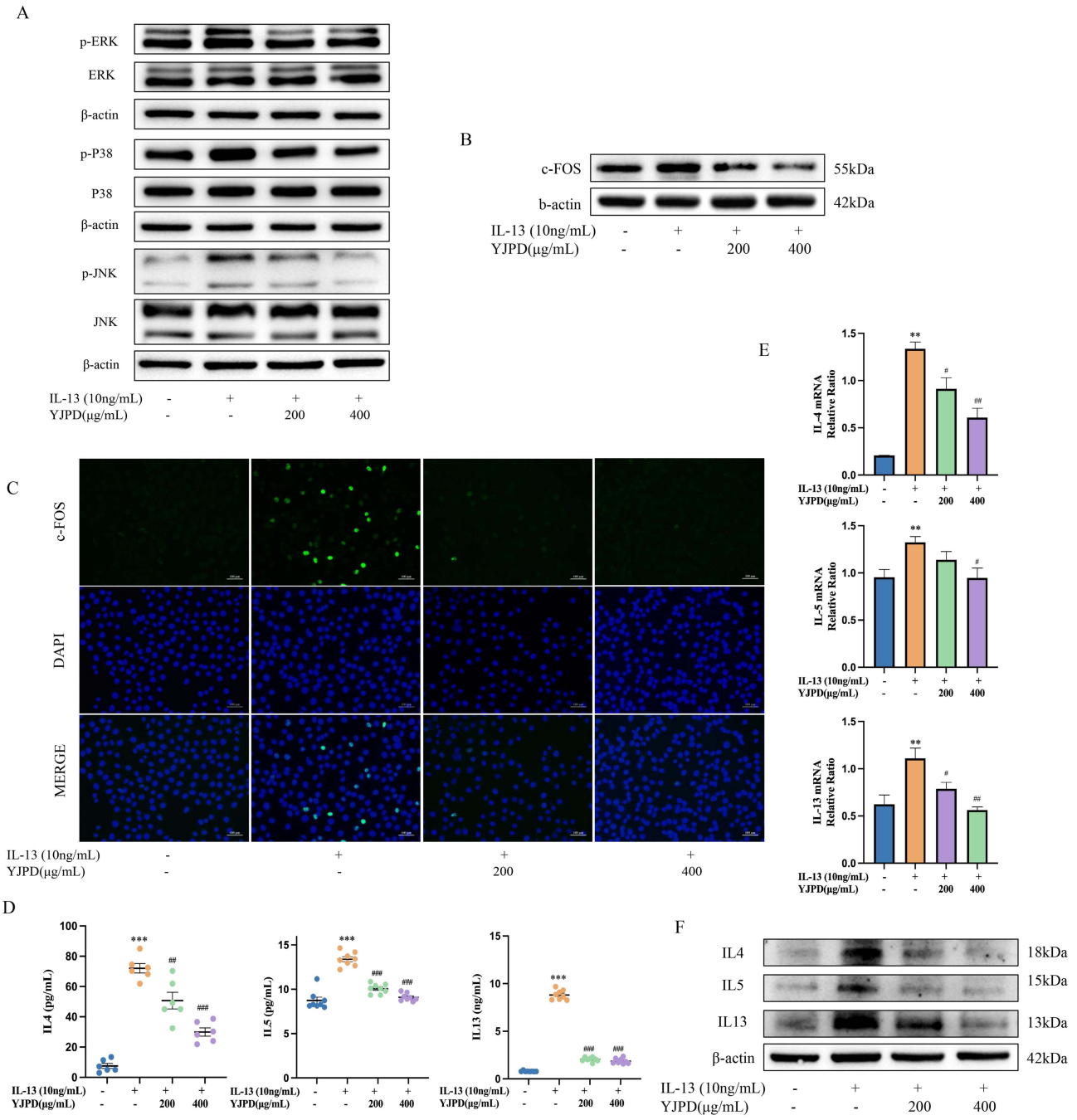

Figure 7 YJPD inhibits inflammatory cytokines via MAPK/AP-1 signaling pathway in HNEpCs. (**A**) Western blots of phospho-ERK1/2, ERK1/2, phospho-P38, P38, phospho-JNK, JNK in IL-13 induced HNEpCs. (**B**) Western blots and (**C**) immunofluorescence of c-FOS in HNEpCs. (**D**) Secretion levels of IL-4, IL-5 and IL-13 in HNEpCs supernatant were detected by Elisa. (**E**) RT-qPCR and Western blot (**F**) of IL-4, IL-5 and IL-13 in HNEpCs. $^{**}p < 0.01$, $^{***}p < 0.001$ versus CON; $^{\#}p < 0.05$, $^{\#\#}p < 0.01$, $^{\#\#\#}p < 0.001$ versus CRSwNP.

IL-4, IL-5, and IL-13 in CRSwNP group were substantially higher than those in the control group and noticeably decreased in YJPD group in a dose-dependent manner. Similarly, in vitro assays also suggested that YJPD can reverse IL13-induced MAPK phosphorylation and relieves inflammation in HNEpCs (Figure 7A–F). These results indicated that YJPD can inhibit the MAPK/AP-1 signaling pathway in CRSwNP.

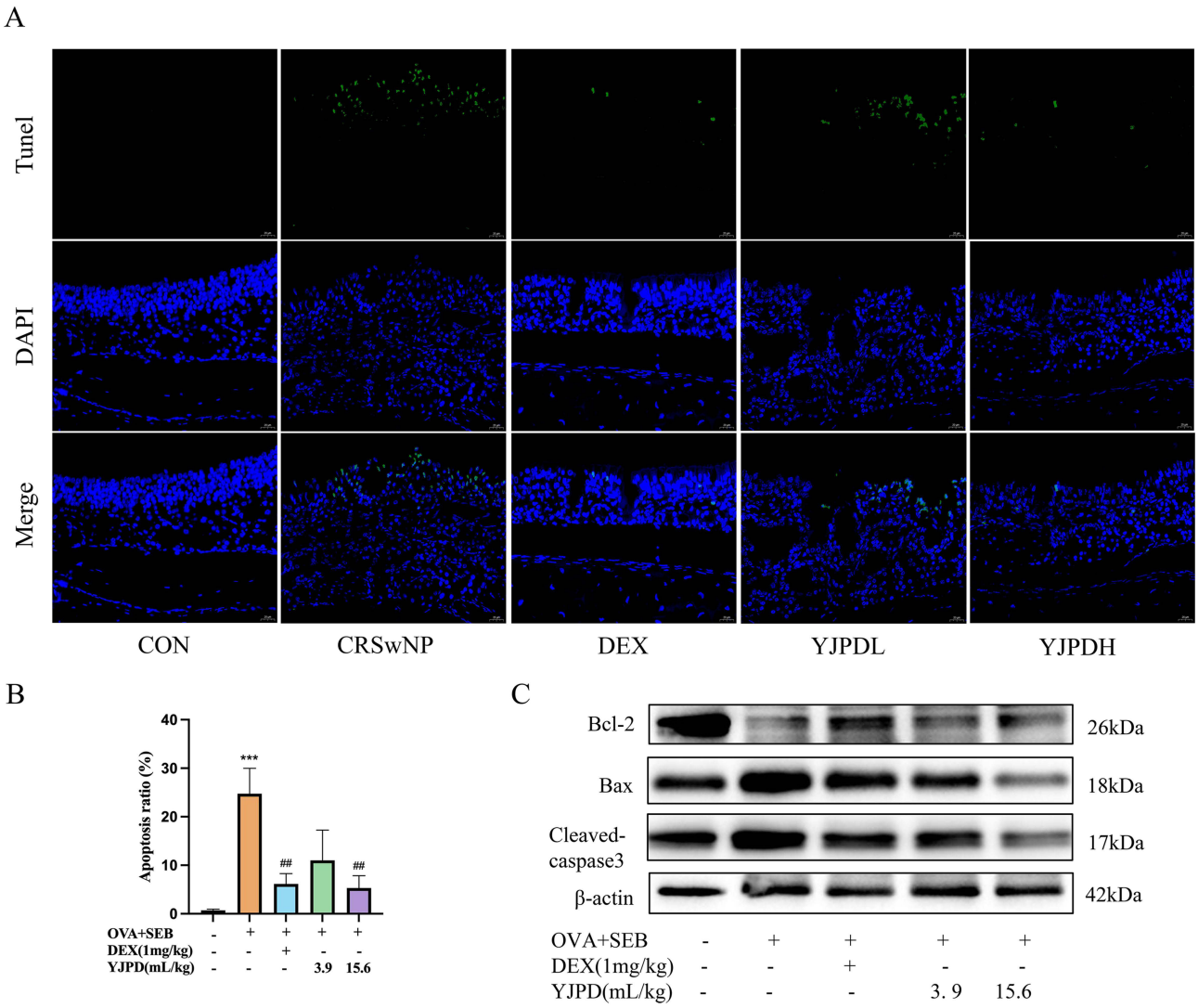

Figure 8 YJPD attenuates apoptosis of nasal epithelial cells in CRSwNP mice. (**A**) Representative images of mouse nasal septal mucosa for Tunel assay (400X). (**B**) The percentage of positive expression of apoptotic cells. (**C**) The expression of apoptosis-related proteins Bcl-2, Bax, Cleaved-caspase3 were determined by Western blot. ***$p < 0.001$ versus CON; ##$p < 0.01$ versus CRSwNP.

YJPD Attenuates Nasal Epithelial Cell Apoptosis

In CRSwNP, excess epithelial apoptosis likely contributes to the severe inflammation of their mucosa. Therefore, we performed TUNEL staining and observed significant apoptosis in the nasal epithelium in the model group, which was significantly attenuated in DEX group and YJPDH groups ($p<0.01$) (Figure 8A and B). However, the inhibition in YJPDL group was not remarkable ($p=0.07$). Furthermore, we detected the levels of several apoptosis-related proteins Bcl-2, Bax, and cleaved caspase-3, and observed that the DEX or YJPD treatment markedly downregulated the levels of Bax, cleaved caspase-3, and upregulated the levels of Bcl-2 in nasal mucosal tissues in CRSwNP mice (Figure 8C).

Correspondingly, we further validated the effect of YJPD on IL-13 induced apoptosis of human nasal mucosal epithelial cells in vitro. Firstly, the apoptosis rate of control group, model group and two drug concentration groups of YJPD were detected by flow cytometry (Figure 9A), and the data showed that the apoptosis rate was 4.9±0.17% in the control group, 19.31±0.36% in the model group, 11.133±0.50% in the YJPD low-dose group and 8.05±0.28% in the YJPD high-dose group (Figure 9B), similar results were obtained by tunel training and Western blot (Figure 9C–E). Together, the above studies suggest that YJPD treatment can relieve apoptosis of nasal mucosal epithelial cells in CRSwNP.

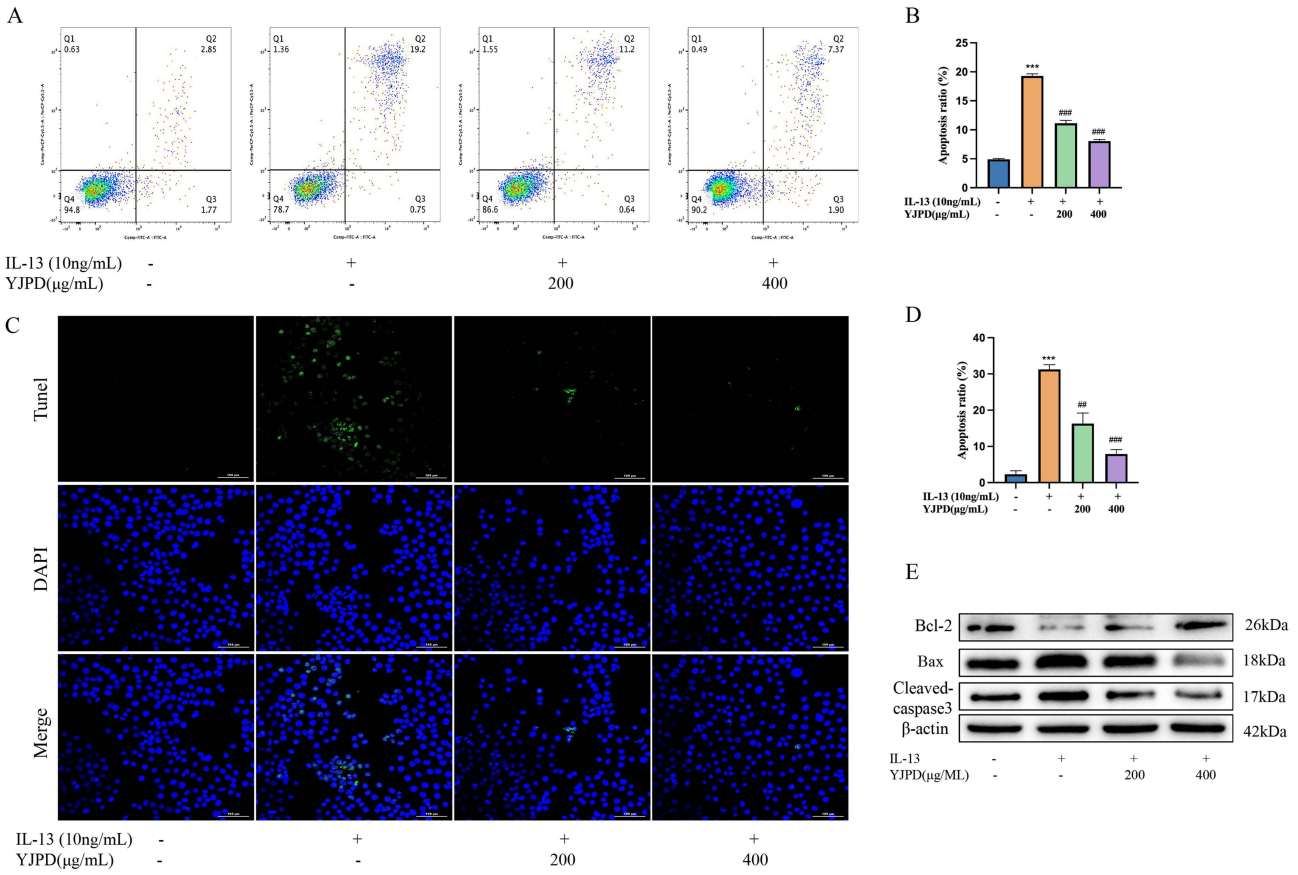

Figure 9 YJPD attenuates IL-13 induced apoptosis in HNEpCs. (**A**) Apoptosis was performed by staining with Annexin V-FITC and PerCP-CY5 and using flow cytometry. (**B**) The apoptosis ratio was analyzed using FlowJo. (**C**) Representative confocal images of HNEpC cells for Tunel tests (400X). (**D**) The percentage of positive expression of apoptotic cells. (**E**) The expression of apoptosis-related proteins Bcl-2, Bax, Cleaved-caspase3 were determined by Western blot. ***$p < 0.001$ versus CON; ##$p < 0.01$, ###$p < 0.001$ versus CRSwNP.

Discussion

The recent European Position Paper on Rhinosinusitis and Nasal Polyps (EPOS) 2020 eliminated the classification of CRSsNP and CRSwNP based on clinical phenotypes, and adopted an intrinsic classification system based on type 2 inflammation (high expression of IL-4, IL-5, and IL-13), and non-type 2 inflammation. Interestingly, CRSwNP patients characterized by type 2 inflammation reflects the importance of reducing specific inflammatory cytokines.[32] New biological treatments (monoclonal antibodies) can block inflammatory pathways and reduce nasal polyp formation in some individuals,[33] but these treatments have not been approved for patients with nasal polyps in China. Therefore, novel therapies are needed to improve disease control. Traditional Chinese believe that the etiology of CRSwNP primarily involves the accumulation of heat and phlegm, thus necessitating a treatment strategy focused on clearing heat, detoxifying and discharging pus. This study we combined network pharmacology, transcriptomics and experiments to substantiate the effectiveness of YJPD and delved into the underlying mechanisms.

Our results showed that YJPD intervention significantly ameliorated symptoms in the OVA+SEB-induced CRSwNP mice. Micro-CT showed that the model group had increased nasal polyp tissue, indicating that the mucous membranes of the nasal cavity and sinuses were inflamed, while the YJPD group could reverse this state to reduced polyps. HE staining showed that YJPD improved nasal mucosal hyperplasia and hypertrophy, epithelial cell morphological changes (such as disordered cell arrangement, ciliated columnar epithelium size and morphology changes, gland proliferation, etc.) and submucosal inflammatory cell infiltration. Patients with CRSwNP frequently exhibit high nasal mucus output and inadequate nasal mucus outflow; moreover, mucus retention in the sinuses and nasal cavity can exacerbate inflammation.

Thus, reducing nasal mucus is an important approach, our PAS staining demonstrated YJPD treatment decreased mucus secretion. These results indicate that the YJPD treats CRSwNP by attenuating nasal mucosal inflammation.

Chronic rhinosinusitis with nasal polyps is induced and perpetuated by cytokines, essentially by the mechanism of the maintenance of a permanent inflammatory status mediated by IL-1β, TNF-α, IL-4, IL-5, IL-13, and IFN-γ, among others.[34] Apparently, these cytokines are involved in TH1 and TH2 cell-driven inflammation. Binding of IL-4 to eosinophils, lymphocytes and monocytes activates inflammatory responses, which plays an important role in the pathogenesis of CRSwNP.[35,36] Tissue inflammation in our mice was induced by OVA and SEB, and both of them are known to increase total IgE production by increasing IL-4 production.[37,38] The present work showed mRNA and protein expression levels of IL-4 in CRSwNP were approximately 15-fold and 20-fold higher than those in the CON group, and a significant reduction in IL-4 expression levels was observed in the mice treated with different concentrations of YJPD. The efficacy of high dose was better than that of low dose, indicating that YJPD inhibited the inflammatory response in a dose-dependent manner. IL-5 is a major regulator of the eosinophil growth, differentiation, migration, and survival, and high levels of IL-5 signify an exaggerated response of Th2 cells.[39] In sinonasal mucosa obtained from OVA+SEB-induced CRSwNP mouse model, significant suppression of the IL-4 and IL-5 level by tofacitinib was identified using ELISA,[40] which was also confirmed by mouse serum samples in our study. IL-13 is an inflammatory cell chemokine, which can regulate the recruitment, homing and activation of inflammatory cells, and then participate in the inflammatory response in allergic reactions.[36] IL-13 can also induce the activation of eosinophils, and promote the expression of adhesion molecules on their surface. IL-13 is significantly highly expressed in patients with CRSwNP, which is involved in the occurrence and development of CRSwNP.[41,42] Therefore, our findings suggest that YJPD reducing the expression levels of Th2 cytokines.

Transcriptomic and network pharmacology analyses have been extensively used to analyze TCM formulas, we combined the results of two methods, obtained that KEGG pathway enrichment focused on the apoptosis and MAPK pathway. As we know, MAPK play a fundamental role in the transcriptional and post-transcriptional regulations of inflammatory genes, T cell differentiation, and cell apoptosis, which mediate airway inflammation;[43,44] and JNK, ERK, and p38 are the three most classical subfamilies of MAPK pathways.[45] Multiple studies have demonstrated that the pro-apoptotic process is mediated by JNK and p38 MAPK cascades, while the regulation of several Bcl-2 proteins occurs at the transcriptional and/or posttranscriptional levels.[46] It is worth noting that ERK1/2 kinases exhibit dual roles in apoptosis. On one hand, they exert anti-apoptotic effects, while on the other hand, under certain conditions, ERK also possesses pro-apoptotic functions, and heightened ERK1/2 signaling can induce tumor cell death.[47] Maxing Shigan Decoction can inhibit airway inflammation in CVA rats by suppressing the activation of TLR4/MyD88/NF-κB and p38 MAPK signaling pathways.[48] In the present study, Western blot analysis of mucosa and HNEpCs showed that YJPD can regulate the MAPK pathway to downregulate the phosphorylation of JNK/ERK/P38.

It is reported that c-FOS had close relevance to MAPK signal pathway. Researches on mucosal inflammatory condition or sinusitis have shown that transcription factor protein-1(AP-1), a downstream factor of MAPK pathway, was activated and translocated to the cell nucleus. AP-1 could transcript some genes, particularly inflammation cytokines (IL-4, IL-5 and GM-CSF), chemokines and adhesion molecules.[49,50] In the present study, Western blotting and immunofluorescence demonstrated that the expression of c-FOS in CRSwNP mice and HNEpCs was higher than that in the control group. This result is in disagreement with those reported by Liu, who showed that IL-13 induces AP-1 related gene c-JUN activation in nasal polyposis. AP-1 also regulates cell apoptosis, T-5224 exerts anti-apoptotic effects by inhibiting the expression of c-FOS protein in lung tissue.[51] Tunel staining was conducted, revealing a notable disparity in the apoptosis of epithelial cells between the experimental and control groups. However, the administration of YJPD exhibited a protective effect on epithelial cells by up-regulating Bcl-2 expression and down-regulating Bax and Cleaved-caspase3 expression.

These findings suggest that YJPD may hold potential as a therapeutic Chinese formula for CRSwNP, and further human studies should be performed to confirm this. In addition, the effects of decoction are not summation of each compound for formula. Therefore, in the future, the key ingredients in YJPD formula should be fully analyzed in detail and its mechanism of action should be deeply penetrated in the hope of providing more accurate treatment solutions for CRSwNP.

Conclusion

The present study demonstrated the therapeutic role of YJPD in CRSwNP and explored its potential mechanism of action. We combined Network Pharmacology, transcriptomics and experiments to verify that YJPD could alleviate inflammation and epithelial apoptosis by inhibiting aberrant activation of the MAPK/AP-1 signaling pathway. This study contributes to the understanding of the mechanisms of YJPD and provides novel therapeutic interventions for CRSwNP.

Abbreviations

CRS, chronic rhinosinusitis; CRSwNP, chronic rhinosinusitis with nasal polyps; DEX, dexamethasone; DEGs, differentially expressed genes; H&E, hematoxylin and eosin; HNEpC, human nasal epithelial cells; HPLC, high-performance liquid chromatography; IgE, immunoglobulin E; IL, interleukin-; MAPK, Mitogen-activated protein kinase; NALF, nasal lavage fluid; OVA, ovalbumin; PAS, periodic acid-Schiff; SEM, scanning electron microscopy; TCMSP, Traditional Chinese Medicine Systems Pharmacology Database and Analysis Platform; Th2, type 2 helper T; TCM, Traditional Chinese medicine; YJPD, Yujiang Paidu decoction.

Ethics Statement

The network pharmacology-based study was reviewed by the Ethics Committee in Yongchuan Chinese Medicine Hospital Affiliated to Chongqing Medical University, and the ethnic approval has been waived. The animal studies were approved by the Institutional Animals Care and Use Committee of Southwest University (Ethics No.: IACUC-20220610-02), and performed in accordance with The Guide for Care and Use of Laboratory Animals released by National Institutes of Health.

Acknowledgments

This work was funded by grants from the Fundamental Research and Frontier Exploration “Overall Rationing System” Project of Chongqing Talent Plan (Grant No. cstc2021ycjh-bg2xm0026), and Chongqing Science and Health Joint Medical Research Project (Grant No. 2022QNXM067).

Disclosure

The authors declare no conflicts of interest in this work.

References

1. Bachert C, Marple B, Schlosser RJ, et al. Adult chronic rhinosinusitis. *Nat Rev Dis Primers*. 2020;6(1):86. doi:10.1038/s41572-020-00218-1
2. Yu J, Yan B, Shen S, et al. IgE directly affects eosinophil migration in CRSwNP through CCR3 and predicts the efficacy of omalizumab. *J Allergy Clin Immunol*. 2023;153:447–460.e9. doi:10.1016/j.jaci.2023.09.041
3. Jin Z, Yan B, Zhang L, Wang C. Current and emerging biological therapies for Chronic rhinosinusitis with nasal polyps with type 2 inflammation. *Expert Opin Investig Drugs*. 2023;32(10):909–919. doi:10.1080/13543784.2023.2273502
4. Fokkens WJ, Lund VJ, Hopkins C, et al. European position paper on rhinosinusitis and nasal polyps 2020. *Rhinology*. 2020;2020:58.
5. Alobid I, Bernal-Sprekelsen M, Mullol J. Chronic rhinosinusitis and nasal polyps: the role of generic and specific questionnaires on assessing its impact on patient’s quality of life. *Allergy*. 2008;63(10):1267–1279. doi:10.1111/j.1398-9995.2008.01828.x
6. Tomassen P, Vandeplas G, Van Zele T, et al. Inflammatory endotypes of chronic rhinosinusitis based on cluster analysis of biomarkers. *J Allergy Clin Immun*. 2016;137(5):1449. doi:10.1016/j.jaci.2015.12.1324
7. Zhang Y, Gevaert E, Lou H, et al. Chronic rhinosinusitis in Asia. *J Allergy Clin Immunol*. 2017;140(5):1230–1239. doi:10.1016/j.jaci.2017.09.009
8. Jiang W-X, Cao -P-P, Li Z-Y, et al. A retrospective study of changes of histopathology of nasal polyps in adult Chinese in central China. *Rhinology*. 2019;57(4):261–267. doi:10.4193/Rhin18.070
9. Yu J, Xian M, Piao Y, Zhang L, Wang C. Changes in clinical and histological characteristics of nasal polyps in Northern China over the past 2-3 decades. *Int Arch Allergy Immunol*. 2021;182(7):615–624. doi:10.1159/000513312
10. Ordovas-Montanes J, Dwyer DF, Nyquist SK, et al. Allergic inflammatory memory in human respiratory epithelial progenitor cells. *Nature*. 2018;560:649–654. doi:10.1038/s41586-018-0449-8
11. Gevaert P, Saenz R, Corren J, et al. Long-term efficacy and safety of omalizumab for nasal polyposis in an open-label extension study. *J Allergy Clin Immunol*. 2022;149(3):957–965e3. doi:10.1016/j.jaci.2021.07.045
12. Yap L, Pothula VB, Warner J, Akhtar S, Yates E. The root and development of otorhinolaryngology in traditional Chinese medicine. *Eur Arch Otorhinolaryngol*. 2009;266(9):1353–1359. doi:10.1007/s00405-009-1041-5
13. Zhao Y, Woo KS, Ma KH, et al. Treatment of perennial allergic rhinitis using Shi-Bi-Lin, a Chinese herbal formula. *J Ethnopharmacol*. 2009;122(1):100–105. doi:10.1016/j.jep.2008.12.005

14. Zhao Y, van Hasselt CA, Woo JK, et al. Effect of a Chinese herbal formula, Shi-Bi-Lin, on an experimental model of allergic rhinitis. *Ann Allerg Asthma Im*. 2006;96(6):844–850. doi:10.1016/S1081-1206(10)61348-8
15. Shingnaisui K, Dey T, Manna P, Kalita J. Therapeutic potentials of Houttuynia cordata Thunb. against inflammation and oxidative stress: a review. *J Ethnopharmacol*. 2018;220:35–43. doi:10.1016/j.jep.2018.03.038
16. Gong L, Zou W, Zheng K, Shi B, Liu M. The Herba Patriniae (Caprifoliaceae): a review on traditional uses, phytochemistry, pharmacology and quality control. *J Ethnopharmacol*. 2021;265:113264. doi:10.1016/j.jep.2020.113264
17. Liao H, Ye J, Gao L, Liu Y. The main bioactive compounds of Scutellaria baicalensis Georgi. for alleviation of inflammatory cytokines: a comprehensive review. *Biomed Pharmacother*. 2021;133:110917. doi:10.1016/j.biopha.2020.110917
18. Li M, Fan X, Zhou L, Jiang M, Shang E. The effect of Ma-Xin-Gan-Shi decoction on asthma exacerbated by respiratory syncytial virus through regulating TRPV1 channel. *J Ethnopharmacol*. 2022;291:115157. doi:10.1016/j.jep.2022.115157
19. Zhao H, Feng YL, Wang M, Wang JJ, Liu T, Yu J. The Angelica dahurica: a Review of Traditional Uses, Phytochemistry and Pharmacology. *Front Pharmacol*. 2022;13:896637. doi:10.3389/fphar.2022.896637
20. Ran X, Ma L, Peng C, Zhang H, Qin LP. Ligusticum chuanxiong Hort: a review of chemistry and pharmacology. *Pharm Biol*. 2011;49 (11):1180–1189. doi:10.3109/13880209.2011.576346
21. Zhang X, Wu XM, Han LH, Qian F, Zhang LQ, Li YM. New furofuran and tetrahydrofuran lignans from the flower buds of Magnolia biondii Pamp and their antiallergic effects. *Nat Prod Res*. 2023;37(18):3083–3092. doi:10.1080/14786419.2022.2147166
22. Jung MA, Song HK, Jo K, et al. Gleditsia sinensis Lam. aqueous extract attenuates nasal inflammation in allergic rhinitis by inhibiting MUC5AC production through suppression of the STAT3/STAT6 pathway. *Biomed Pharmacother*. 2023;161:114482. doi:10.1016/j.biopha.2023.114482
23. Shi G, Kong J, Wang Y, Xuan Z, Xu F. Glycyrrhiza uralensis Fisch. alleviates dextran sulfate sodium-induced colitis in mice through inhibiting of NF-kappaB signaling pathways and modulating intestinal microbiota. *J Ethnopharmacol*. 2022;298:115640. doi:10.1016/j.jep.2022.115640
24. Mao D, Yang Z, Xiao S, He Z, Guo F. Treatment of 86 cases of suppurative sinusitis with Yujiang paidu decoction. *JETCM*. 2011;20(08):1302. doi:10.3969/j.issn.1004-745X.2011.08.052
25. Mao D, Xie H, Zhang F, Li L, She H. Yu Jiang detoxification mixture douches the nasal sinus in patients with chronic nasal sinusitis curative effect observation. *J Chin Ophthalmol & Otorhinolaryngol*. 2017;7(2):92–95. doi:10.3969/j.issn.1674-9006.2017.02.011
26. Li Q. *Pathologic observation and immune mechanism of Yujiang paidu decoction in treatment of chronic sinusitis*. [Master Dissertation]. Chongqing Medical University; 2022.
27. Zhang W, Tian W, Wang Y, et al. Explore the mechanism and substance basis of Mahuang FuziXixin Decoction for the treatment of lung cancer based on network pharmacology and molecular docking. *Comput Biol Med*. 2022;151(Pt A):106293. doi:10.1016/j.compbiomed.2022.106293
28. Choi MR, Xu J, Lee S, et al. Chloroquine treatment suppresses mucosal inflammation in a mouse model of eosinophilic chronic rhinosinusitis. *Allergy Asthma Immunol Res*. 2020;12(6):994–1011. doi:10.4168/aair.2020.12.6.994
29. Dunston D, Ashby S, Krosnowski K, Ogura T, Lin W. An effective manual deboning method to prepare intact mouse nasal tissue with preserved anatomical organization. *J Vis Exp*. 2013;(78). doi:10.3791/50538
30. Zhang Y, Song Y, Wang C, et al. Panax notoginseng saponin R1 attenuates allergic rhinitis through AMPK/Drp1 mediated mitochondrial fission. *Biochem Pharmacol*. 2022;202:115106. doi:10.1016/j.bcp.2022.115106
31. Zhong B, Seah J Jie, Liu F, Ba L, Du J, Wang D Yun. (2022). The role of hypoxia in the pathophysiology of chronic rhinosinusitis. Allergy, 77(11), 3217–3232. 10.1111/all.15384
32. Wang W, Xu Y, Wang L, et al. Single-cell profiling identifies mechanisms of inflammatory heterogeneity in chronic rhinosinusitis. *Nat Immunol*. 2022;23(10):1484–1494. doi:10.1038/s41590-022-01312-0
33. Bachert C, Han JK, Desrosiers M, et al. Efficacy and safety of dupilumab in patients with severe chronic rhinosinusitis with nasal polyps (LIBERTY NP SINUS-24 and LIBERTY NP SINUS-52): results from two multicentre, randomised, double-blind, placebo-controlled, parallel-group Phase 3 trials. *Lancet*. 2019;394(10209):1638–1650. doi:10.1016/S0140-6736(19)31881-1
34. Kato A, Schleimer RP, Bleier BS. Mechanisms and pathogenesis of chronic rhinosinusitis. *J Allergy Clin Immunol*. 2022;149(5):1491–1503. doi:10.1016/j.jaci.2022.02.016
35. Izuhara K, Nunomura S, Nanri Y, et al. Periostin in inflammation and allergy. *Cell Mol Life Sci*. 2017;74(23):4293–4303. doi:10.1007/s00018-017-2648-0
36. Santini G, Mores N, Malerba M, et al. Dupilumab for the treatment of asthma. *Expert Opin Investig Drugs*. 2017;26(3):357–366. doi:10.1080/13543784.2017.1282458
37. Spiegelberg HL. The role of interleukin-4 in IgE and IgG subclass formation. *Springer Semin Immunopathol*. 1990;12(4):365–383. doi:10.1007/BF00225324
38. Chegini Z, Didehdar M, Khoshbayan A, Karami J, Yousefimashouf M, Shariati A. The role of Staphylococcus aureus enterotoxin B in chronic rhinosinusitis with nasal polyposis. *Cell Commun Signal*. 2022;20(1):29. doi:10.1186/s12964-022-00839-x
39. Haddad EB, Cyr SL, Arima K, McDonald RA, Levit NA, Nestle FO. Current and emerging strategies to inhibit type 2 inflammation in atopic dermatitis. *Dermatol Ther*. 2022;12(7):1501–1533. doi:10.1007/s13555-022-00737-7
40. Joo YH, Cho HJ, Jeon YJ, et al. Therapeutic effects of intranasal tofacitinib on chronic rhinosinusitis with nasal polyps in mice. *Laryngoscope*. 2021;131(5):E1400–E1407. doi:10.1002/lary.29129
41. Gandhi NA, Bennett BL, Graham NM, Pirozzi G, Stahl N, Yancopoulos GD. Targeting key proximal drivers of type 2 inflammation in disease. *Nat Rev Drug Discov*. 2016;15(1):35–50. doi:10.1038/nrd4624
42. Lin YT, Lin CF, Liao CK, Yeh TH. Comprehensive evaluation of type 2 endotype and clinical features in patients with chronic rhinosinusitis with nasal polyps in Taiwan: a cross-sectional study. *Eur Arch Otorhinolaryngol*. 2023;280(12):5379–5389. doi:10.1007/s00405-023-08118-2
43. Khorasanizadeh M, Eskian M, Gelfand EW, Rezaei N. Mitogen-activated protein kinases as therapeutic targets for asthma. *Pharmacol Ther*. 2017;174:112–126. doi:10.1016/j.pharmthera.2017.02.024
44. Qin D, Liu P, Zhou H, et al. TIM-4 in macrophages contributes to nasal polyp formation through the TGF-beta1-mediated epithelial to mesenchymal transition in nasal epithelial cells. *Front Immunol*. 2022;13:941608. doi:10.3389/fimmu.2022.941608
45. Johnson GL, Lapadat R. Mitogen-activated protein kinase pathways mediated by ERK, JNK, and p38 protein kinases. *Science*. 2002;298 (5600):1911–1912. doi:10.1126/science.1072682

46. Garcia-Fernandez LF, Losada A, Alcaide V, et al. Aplidin induces the mitochondrial apoptotic pathway via oxidative stress-mediated JNK and p38 activation and protein kinase C delta. *Oncogene*. 2002;21(49):7533–7544. doi:10.1038/sj.onc.1205972
47. Sugiura R, Satoh R, Takasaki T. ERK: a double-edged sword in cancer. ERK-dependent apoptosis as a potential therapeutic strategy for cancer. *Cells*. 2021;10(10):2509. doi:10.3390/cells10102509
48. Fu Z, Zhou L, Zhang B-L. Effect and mechanism of Maxing Shigan Decoction on reducing inflammatory response in rats with cough variant asthma via TLR4/MyD88/NF-κB and p38 MAPK signaling pathways. *China J Chinese Materia Medica*. 2023;48:1–9. doi:10.19540/j.cnki.cjcmm.20230921.406
49. Necela BM, Cidlowski JA. Mechanisms of glucocorticoid receptor action in noninflammatory and inflammatory cells. *Proc Am Thorac Soc*. 2004;1(3):239–246. doi:10.1513/pats.200402-005MS
50. Valera FC, Queiroz R, Scrideli C, Tone LG, Anselmo-Lima WT. Expression of transcription factors NF-kappaB and AP-1 in nasal polyposis. *Clin Exp Allergy*. 2008;38(4):579–585. doi:10.1111/j.1365-2222.2007.02929.x
51. Zhou L, Xue C, Chen Z, Jiang W, He S, Zhang X. c-Fos is a mechanosensor that regulates inflammatory responses and lung barrier dysfunction during ventilator-induced acute lung injury. *BMC Pulm Med*. 2022;22(1):9. doi:10.1186/s12890-021-01801-2